EPJ Web of Conferences **146**, 03020 (2017) DOI: 10.1051/epjconf/201714603020
ND2016

Characterization of the n_TOF EAR-2 neutron beam

Y.H. Chen[1,a], L. Tassan-Got[1], L. Audouin[1], C. Le Naour[1], I. Durán[2], E. Casarejos[3], O. Aberle[4], J. Andrzejewski[5], V. Bécares[6], M. Bacak[7], J. Balibrea[6], M. Barbagallo[8], S. Barros[9], F. Bečvář[10], C. Beinrucker[11], E. Berthoumieux[12], J. Billowes[13], D. Bosnar[14], M. Brugger[4], M. Caamaño[2], F. Calviño[15], M. Calviani[4], D. Cano-Ott[6], R. Cardella[4], A. Casanovas[15], D.M. Castelluccio[16,17], F. Cerutti[4], E. Chiaveri[4], N. Colonna[8], G. Cortés[15], M.A. Cortés-Giraldo[18], L. Cosentino[19], L.A. Damone[8,20], M. Diakaki[12], C. Domingo-Pardo[21], R. Dressler[22], E. Dupont[12], B. Fernández-Domínguez[2], A. Ferrari[4], P. Ferreira[9], P. Finocchiaro[19], V. Furman[23], K. Göbel[11], M.B. Gómez-Hornillos[15], A.R. García[6], A. Gawlik[5], T. Glodariu[24], I.F. Gonçalves[9], E. González[6], A. Goverdovski[25], E. Griesmayer[7], C. Guerrero[18], F. Gunsing[12,4], H. Harada[26], T. Heftrich[11], S. Heinitz[22], J. Heyse[27], D.G. Jenkins[28], E. Jericha[7], F. Käppeler[29], Y. Kadi[4], T. Katabuchi[30], P. Kavrigin[7], V. Ketlerov[25], V. Khryachkov[25], A. Kimura[26], N. Kivel[22], M. Kokkoris[31], M. Krtička[10], E. Leal-Cidoncha[2], C. Lederer[32], H. Leeb[7], J. Lerendegui-Marco[18], S. Lo Meo[16,17], S.J. Lonsdale[32], R. Losito[4], D. Macina[4], J. Marganiec[5], T. Martínez[6], C. Massimi[17,33], P. Mastinu[34], M. Mastromarco[8], F. Matteucci[35,36], E.A. Maugeri[22], E. Mendoza[6], A. Mengoni[16], P.M. Milazzo[35], F. Mingrone[17], M. Mirea[24], S. Montesano[4], A. Musumarra[19,37], R. Nolte[38], A. Oprea[24], N. Patronis[39], A. Pavlik[40], J. Perkowski[5], J.I. Porras[4,41], J. Praena[18,41], J.M. Quesada[18], K. Rajeev[42], T. Rauscher[43,44], R. Reifarth[11], A. Riego-Perez[15], M. Robles[2], P.C. Rout[42], C. Rubbia[4], J.A. Ryan[13], M. Sabaté-Gilarte[4,18], A. Saxena[42], P. Schillebeeckx[27], S. Schmidt[11], D. Schumann[22], P. Sedyshev[23], A.G. Smith[13], A. Stamatopoulos[31], G. Tagliente[8], J.L. Tain[21], A. Tarifeño-Saldivia[21], A. Tsinganis[31], S. Valenta[10], G. Vannini[17,33], V. Variale[8], P. Vaz[9], A. Ventura[17], V. Vlachoudis[4], R. Vlastou[31], A. Wallner[45], S. Warren[13], M. Weigand[11], C. Weiss[4,7], C. Wolf[11], P.J. Woods[32], T. Wright[13], P. Žugec[14,4], and the n_TOF Collaboration

[1] Institut de Physique Nucléaire, CNRS-IN2P3, Univ. Paris-Sud, Université Paris-Saclay, 91406 Orsay Cedex, France
[2] University of Santiago de Compostela, Spain
[3] University of Vigo, Spain
[4] European Organization for Nuclear Research (CERN), Switzerland
[5] University of Lodz, Poland
[6] Centro de Investigaciones Energeticas Medioambientales y Tecnológicas (CIEMAT), Spain
[7] Technische Universität Wien, Austria
[8] Istituto Nazionale di Fisica Nucleare, Sezione di Bari, Italy
[9] Instituto Superior Técnico, Lisbon, Portugal
[10] Charles University, Prague, Czech Republic
[11] Goethe University Frankfurt, Germany
[12] CEA Saclay, Irfu, Gif-sur-Yvette, France
[13] University of Manchester, UK
[14] University of Zagreb, Croatia
[15] Universitat Politècnica de Catalunya, Spain
[16] Agenzia nazionale per le nuove tecnologie (ENEA), Bologna, Italy
[17] Istituto Nazionale di Fisica Nucleare, Sezione di Bologna, Italy
[18] Universidad de Sevilla, Spain
[19] INFN Laboratori Nazionali del Sud, Catania, Italy
[20] Dipartimento di Fisica, Università degli Studi di Bari, Italy
[21] Instituto de Física Corpuscular, Universidad de Valencia, Spain
[22] Paul Scherrer Institut (PSI), Villingen, Switzerland
[23] Joint Institute for Nuclear Research (JINR), Dubna, Russia
[24] Horia Hulubei National Institute of Physics and Nuclear Engineering, Romania
[25] Institute of Physics and Power Engineering (IPPE), Obninsk, Russia
[26] Japan Atomic Energy Agency (JAEA), Tokai-mura, Japan
[27] European Commission, Joint Research Centre, Geel, Retieseweg 111, 2440 Geel, Belgium
[28] University of York, UK
[29] Karlsruhe Institute of Technology, Campus North, IKP, 76021 Karlsruhe, Germany
[30] Tokyo Institute of Technology, Japan
[31] National Technical University of Athens, Greece
[32] School of Physics and Astronomy, University of Edinburgh, UK

[a] e-mail: yonghao.chen@cern.ch

[33] Dipartimento di Fisica e Astronomia, Università di Bologna, Italy
[34] Istituto Nazionale di Fisica Nucleare, Sezione di Legnaro, Italy
[35] Istituto Nazionale di Fisica Nucleare, Sezione di Trieste, Italy
[36] Dipartimento di Astronomia, Università di Trieste, Italy
[37] Dipartimento di Fisica e Astronomia, Università di Catania, Italy
[38] Physikalisch-Technische Bundesanstalt (PTB), Bundesallee 100, 38116 Braunschweig, Germany
[39] University of Ioannina, Greece
[40] University of Vienna, Faculty of Physics, Vienna, Austria
[41] University of Granada, Spain
[42] Bhabha Atomic Research Centre (BARC), India
[43] Centre for Astrophysics Research, University of Hertfordshire, UK
[44] Department of Physics, University of Basel, Switzerland
[45] Australian National University, Canberra, Australia

Abstract. The experimental area 2 (EAR-2) at CERNs neutron time-of-flight facility (n_TOF), which is operational since 2014, is designed and built as a short-distance complement to the experimental area 1 (EAR-1). The Parallel Plate Avalanche Counter (PPAC) monitor experiment was performed to characterize the beam profile and the shape of the neutron flux at EAR-2. The prompt γ-flash which is used for calibrating the time-of-flight at EAR-1 is not seen by PPAC at EAR-2, shedding light on the physical origin of this γ-flash.

1. Introduction

A second experimental area (EAR-2) at CERN's neutron time-of-flight facility (n_TOF), having a flight path of ~20 m from the spallation lead target and 90 degrees respect to the incoming proton beam, has been designed and built, offering advantages compared with the former experimental area (EAR-1): 1) much higher neutron flux of about a factor 25; 2) for highly radioactive samples an additional factor 10 is obtained for the signal to noise ratio due to shorter time interval resulting from the 10 times shorter flight distance [1,2], thus fulfilling the demands of the neutron science community for a time-of-flight facility with a higher flux [3].

In this contribution we present the characterization of the EAR-2 neutron beam by means of a measurement with the Parallel Plate Avalanche Counter (PPAC).

2. Experimental setup

2.1. n_TOF facility at CERN

The n_TOF facility at CERN is based on a spallation neutron source which can provide neutrons from thermal energy up to GeV by impinging 20 GeV/c protons onto a thick lead target. The proton beam has a typical intensity of 7×10^{12}/pulse with 7 ns (RMS) pulse width and a cycle of 1.2 s or its multiple, yielding about 300 neutrons per single incident proton. The layout of the n_TOF facility is depicted in Fig. 1 showing the two perpendicular neutron beam lines.

The horizontal neutron beam line sends neutrons to EAR-1 through a ~185 m flight path which has a 10 degree angle regarding to the proton beam in the horizontal plane. While EAR-1 is in operation since 2001, the vertical ~20 m beam line associated with EAR-2 has been constructed and is operational since 2014, performing its high neutron flux and attenuated γ-flash as a complement. Detailed technical descriptions of the n_TOF facility can be found in Refs. [4,5].

2.2. PPAC monitor (PPACmon) setup at EAR-2

The PPACs used at n_TOF, which were developed at Institut de Physique Nuclaire d'Orsay (IPNO) in France [6], are gaseous detectors filled with C_3F_8 (octafluoropropane) and working at around 4 mbar typically. Each PPAC consists of a central anode used for timing measurements and two cathodes on each side of the anode for localization with a resolution of 2 mm. The active surface is 200 mm × 200 mm, and the overall assembled dimensions of a PPAC are 305 mm × 305 mm and 13 mm in thickness. Several PPAC detectors can be arranged with interleaved targets, in different experiment configurations.

A new chamber, called PPACmon, was designed and constructed by IPNO, jointly with the University of Santiago de Compostela (Spain) and CERN. As sketched in Fig. 2, the configuration used in EAR-2 consists of 3 PPACs and 2 ^{235}U targets perpendicular to the neutron beam. Each ^{235}U target deposited on a 0.7 μm aluminium

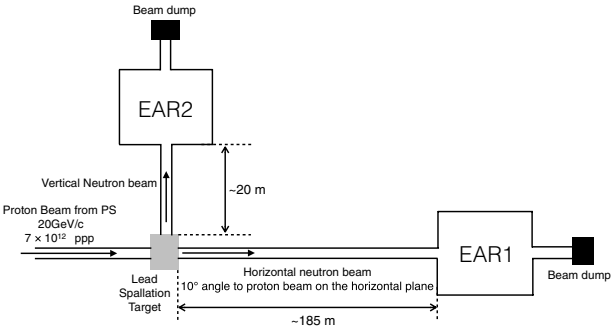

Figure 1. Layout of the n_TOF facility.

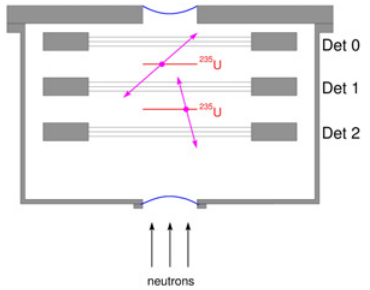

Figure 2. PPAC monitor setup at n_TOF EAR-2.

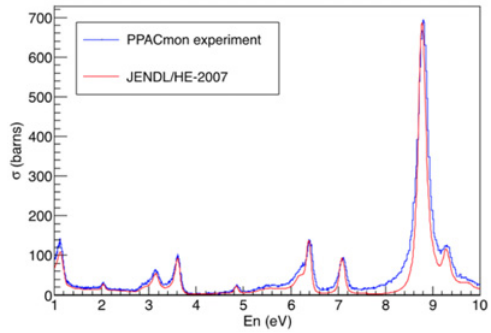

Figure 3. Comparison of the experimental fission rate and ^{235}U(n,f) cross section in the database.

backing with a thickness of ~70 μg/cm^2 is surrounded by 2 PPACs, so that fission events can be selected by the coincident detection of the fission fragments. This coincidence method is highly selective on fission reactions, rejecting radioactive emissions and more importantly other spallation reactions above tens of MeV.

3. Results and discussions

3.1. Energy determination

The incident neutron energy is determined by the velocity

$$v \propto \frac{L}{T - T_0} \tag{1}$$

where L is the flight path, T is the time recorded by the detector and T_0 is the starting flight time. So $T - T_0$ is the time-of-flight (TOF). Among these 3 parameters, only T is precisely known which is directly given by the anode of the PPAC. L and T_0 need to be determined.

L is obtained by the comparison of the detected fission rate and the standard $^{235}U(n, f)$ cross section [7] in the resonance region where T is large enough that T_0 can be neglected and we can use T instead of TOF. We adjust L for obtaining the best match with the JENDL/HE-2007 database [7] (Fig. 3).

T_0 is usually determined by the prompt γ-flash signal which is a sharp narrow peak at the beginning of the signal frame in case of the measurement at EAR-1. But this method is not applicable here since the sharp peak is not visible at EAR-2. Instead, we use the pickup (PK) signal of proton beam as the time reference to determine T_0. Because the PK signal is delayed compared with the true T_0, an offset is added to determine TOF. The offset is determined based both on the simulation and the first fission event of each proton pulse which could be induced by photons or other high energy particles.

$$TOF \propto T - PK + Offset \tag{2}$$

The TOF spectrum with 100 bins per decade (bpd) is shown in Fig. 4 and the fission rate as a function of neutron energy with 100 bpd is shown in Fig. 5.

3.2. Beam profile reconstruction

The position distributions of the fission fragments on PPAC 1 and PPAC 2 (Det 1 and Det 2 in Fig. 2) are shown in Figs. 6 and 7. In Fig. 7 there is a distorted region around −20 mm ≤ X ≤ 40 mm and −20 mm ≤ Y ≤ 20 mm, probably due to a hardware problem of PPAC 2 during the experiment.

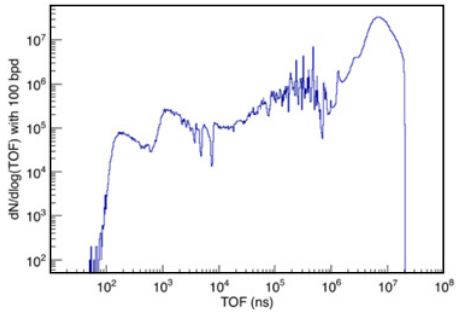

Figure 4. Neutron TOF spectrum with 100 bpd.

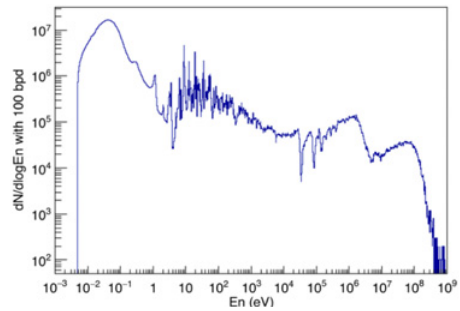

Figure 5. The fission rate as a function of neutron energy with 100 bpd.

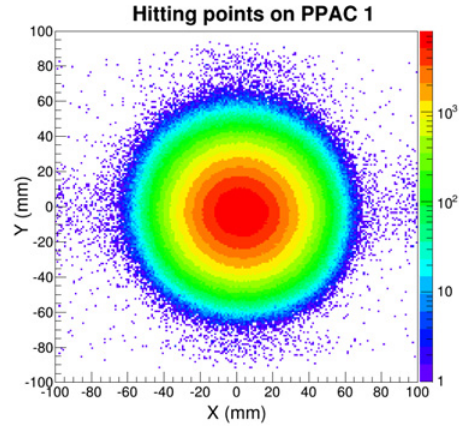

Figure 6. Fission fragment distribution on PPAC 1.

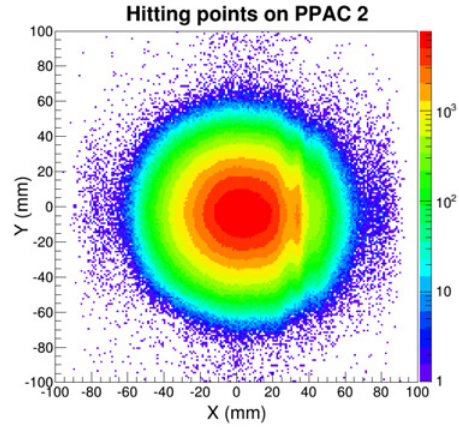

Figure 7. Fission fragment distribution on PPAC 2.

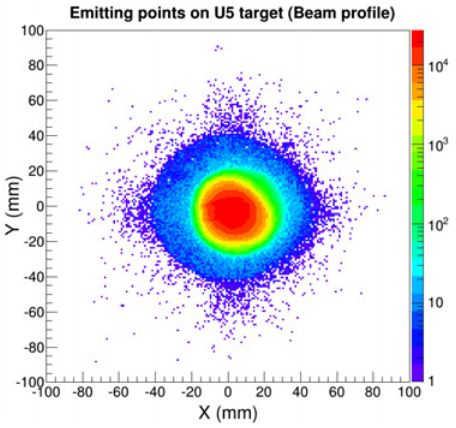

Figure 8. Neutron beam profile at n_TOF EAR-2.

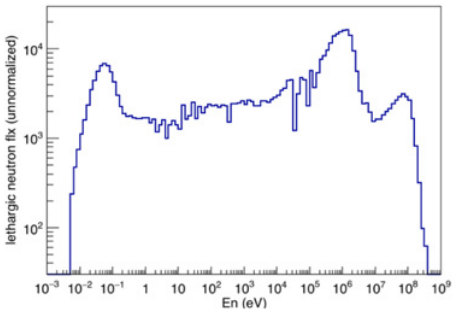

Figure 9. Unnormalized lethargic neutron flux at n_TOF EAR-2 obtained with the PPACmon.

The beam profile (Fig. 8), i.e. the emitting points on the target between PPAC 1 and PPAC 2, can be reconstructed according to Figs. 6 and 7 based on the back to back emission of fission fragments.

3.3. Neutron flux

The energy dependence of the neutron flux can be obtained by dividing the fission rate (Fig. 5) by the ^{235}U(n,f) cross section [7]. For neutrons above 1 MeV, the fission fragment angular distribution (FFAD) is not isotropic any more due to the momentum transfer from the incident neutrons to the target nuclei. The anisotropy correction is applied in the calculation of the neutron flux above 1 MeV based on the FFAD of ^{235}U from a PPAC measurement in 2011 [8]. The unnormalized energy dependence of the lethargic neutron flux is shown in Fig. 9.

The unnormalized preliminary result in Fig. 9 shows that PPACs are covering a wide energy range, extending to very high energies. A more dedicated and specific work for the evaluation of EAR-2 neutron flux by the n_TOF collaboration which will be published soon.

4. Conclusions

We present the first PPACmon experiment, done at n_TOF EAR-2, for characterizing the beam profile and neutron flux at this new facility. We also found that the prompt γ-flash signal (sharp narrow peak with a high amplitude) is not visible at EAR-2, contrary to EAR-1. It means that the these prompt γ-flash is not caused by the deexcitation of nuclei in the spallation target but from the angle focused in-flight decay of high velocity particles which follow the horizontal beam line and are, therefore, excluded from the vertical beam line to EAR-2. Geant4 simulation indicates that prompt γ-rays are essentially from the decay of neutral pions (π^0), with π^0s coming from nucleon-nucleon collision in intranuclear cascades. Since π^0s are highly boosted forward along the proton beam in laboratory frame, so are the γ-rays, which means they can follow the horizontal beam line to EAR-1 but only very litte can fly to EAR-2. The deexcitation of the nuclei in the lead target and neutron capture in lead and moderation layer can produce both prompt and delayed γ-rays, results in a broad γ-flash lasting up to a few hundred nanoseconds. This is quasi isotropic and visible both at EAR-1 and EAR-2.

The USC group contribution has been partly supported by Spanish grant FPA2013-46236-P.

References

[1] Chiaveri, E. Proposal for n_TOF Experimental Area 2. No. CERN-INTC-2012-029, 2012
[2] Gunsing, F., et al. Nuclear data measurements at the upgraded neutron time-of-flight facility n_TOF at CERN. 14th International Conference on Nuclear Reaction Mechanisms, 2015
[3] Bracco, A., et al. *Perspectives of Nuclear Physics in Europe: NuPECC Long Range Plan 2010* (European Science Foundation, 2010), 142
[4] Berthoumieux, E. et al., The neutron Time-Of-Flight facility n_TOF at CERN (I): Technical Description, CERN n TOF Public Note n TOF-PUB-2013-001 (2013)
[5] Weiss, C., et al. The new vertical neutron beam line at the CERN n_TOF facility design and outlook on the performance. NIMA **799**, 90 (2015)
[6] Stephan, C., et al. Neutron-Induced Fission Cross Section Measurements between 1 eV and 250 MeV. Journal of Nucl. Sci. Tech. **39**(sup2), 276–279 (2002)
[7] Fukahori, T., Konobeyev, A.Yu. JENDL/HE-2007
[8] Leong, L.S. *Fission fragment angular distribution and fission cross section validation*(Doctoral dissertation, Universit Paris Sud-Paris XI) (2013)